

Mechanical alloying in the Al–Bi alloy system

KEISUKE UENISHI, KIM HA YONG*, KOJIRO F. KOBAYASHI

Department of Welding and Production Engineering, Faculty of Engineering, Osaka University, Yamadaoka 2-1, Suita, Osaka 565, Japan and

()Department of Metallurgical Engineering, Taejon National University of Technology, Dong-ku, Taejon, Korea*

Mechanical alloying (MA) was carried out to investigate the MA behaviour of the immiscible Al–10, 30 at % Bi alloys. After the MA processing, the Al and Bi were finely and homogeneously alloyed. The Bi crystallite size decreased to 25 nm and 30 nm in the Al–10 at % Bi and Al–30 at % Bi alloys, respectively. By increasing the MA time, the hardness increased up to a value of 80 H_v , which is larger than that obtained from the rule of mixtures. The lattice parameter of Bi decreased by about 0.27%, which shows the formation of a non-equilibrium hcp Bi super-saturated solid solution. The extended solubility of Al in Bi was 1.9% in the Al–30 at % Bi alloy. Due to the extended solubility, depression of the melting temperature of hcp Bi was confirmed in the mechanically alloyed Al–Bi alloys. The maximum depression in the temperature was about 10 K. The measured values corresponded well with those estimated from the extrapolation of the solidus line.

1. Introduction

The mechanical alloying (MA) process is a new method of powder metallurgy for producing composite metal powders with a controlled microstructure. MA was developed as a means for combining the advantages of gamma prime (γ') precipitation hardening and oxide dispersion strengthening (ODS) in the Ni based alloy IN-853 [1]. It is also applicable to a larger number of alloy systems [2], which are difficult or impossible to produce by conventional melting and casting techniques (IM) due to segregation, high melting temperature or very high reactivity with crucibles. The interdispersion process of the ingredients by MA is not due to a simple mixing of the powders, but to a cold welding and fracturing of the elemental powder mixture in the solid state.

Moreover, Koch *et al.* [3] have suggested that MA can substantially alter structures at the atomic level. Firstly, in a Ni–Nb alloy system with negative heat of mixing, an amorphous phase was formed by MA of the elemental mixture. After that report, the formation of amorphous [4], non-equilibrium crystal [5], or equilibrium crystal [6] phases were confirmed in many alloy systems with a negative heat of mixing.

In the alloy systems with a positive heat of mixing, there is a repulsive interaction between elements, so they hardly form compounds or solid solutions. Moreover, it is difficult to even prepare a finely mixed alloy by conventional casting. However, by the application of the MA technique, a nano ordered mixed alloy can be prepared [7]. Recently, even in such alloy systems, it has been confirmed that MA can induce a crystal structural change [8–10]. In the alloy systems, there

are no apparent driving forces for the formation of non-equilibrium phases due to the repulsive force between ingredients. However, nano ordered mixing of ingredients was accomplished by MA, which raised the free energy of the alloy system by the increase of grain boundary energy and thus created the driving force.

In this present study, we report the MA behaviour in Al–Bi alloys with a positive heat of mixing ($\Delta H = 50$ kJ/mol).

The characteristics of the Al–Bi system are as follows.

(1) The two elements are mutually insoluble in the solid state.

(2) The crystal structures of Al and Bi are fcc and hcp, respectively. There is a large difference (27%) in their atomic radii.

(3) There is a monotectic reaction with a region of immiscibility below 1310 K which extends down to 948 K from 0.002–84.0 at % Bi, and a eutectic reaction which extends from 0–100 at % Bi at 543 K in the phase diagram.

In previous work in the Al–In alloy system, which is a similar alloy system to Al–Bi, the alloying behaviour with MA was investigated and the formation of non-equilibrium phases was presented [11]. In the Al–Bi system, too, it is expected that new non-equilibrium phases will be formed and that a depression in the melting temperature will occur. In the current study changes in the structure and hardness were investigated as a function of MA time or alloying composition. X-ray diffraction and differential scanning calorimetry analyses were performed to identify the phases formed by MA.

2. Experimental procedure

The elemental Al (purity 99.8% and particle size 20 μm) and Bi (purity 99.99% and particle size 50–100 μm) were mixed to give the average composition of Al-10 at % Bi or Al-30 at % Bi. The mixed powders were put into a cylindrical stainless steel container with stainless steel balls under an atmosphere of 99.99% pure argon. The container and balls used for milling were made of SUS 304 stainless steel. The size of the container was 55 mm inner diameter and 40 mm in height. The balls were 9 mm in diameter. The ball-to-powder weight ratio was fixed to 36:1. To avoid the adhesion of powder to the

balls and vial, about 0.55 cc of ethanol was added to the sample powder as a process control agent (PCA).

MA was performed using a vibrating ball mill (Nishin Gikken, Misumi, NEV-MA8, vibrating frequency; 13.1 Hz). To follow the changes in the powders during the MA, the powders were mechanically alloyed for various times without any intervals.

X-ray diffraction analyses using $\text{CoK}\alpha$ radiation were performed to identify the phases formed by MA. The microstructure of powders obtained was observed by scanning electron microscopy (SEM) and transmission electron microscopy (TEM). For TEM

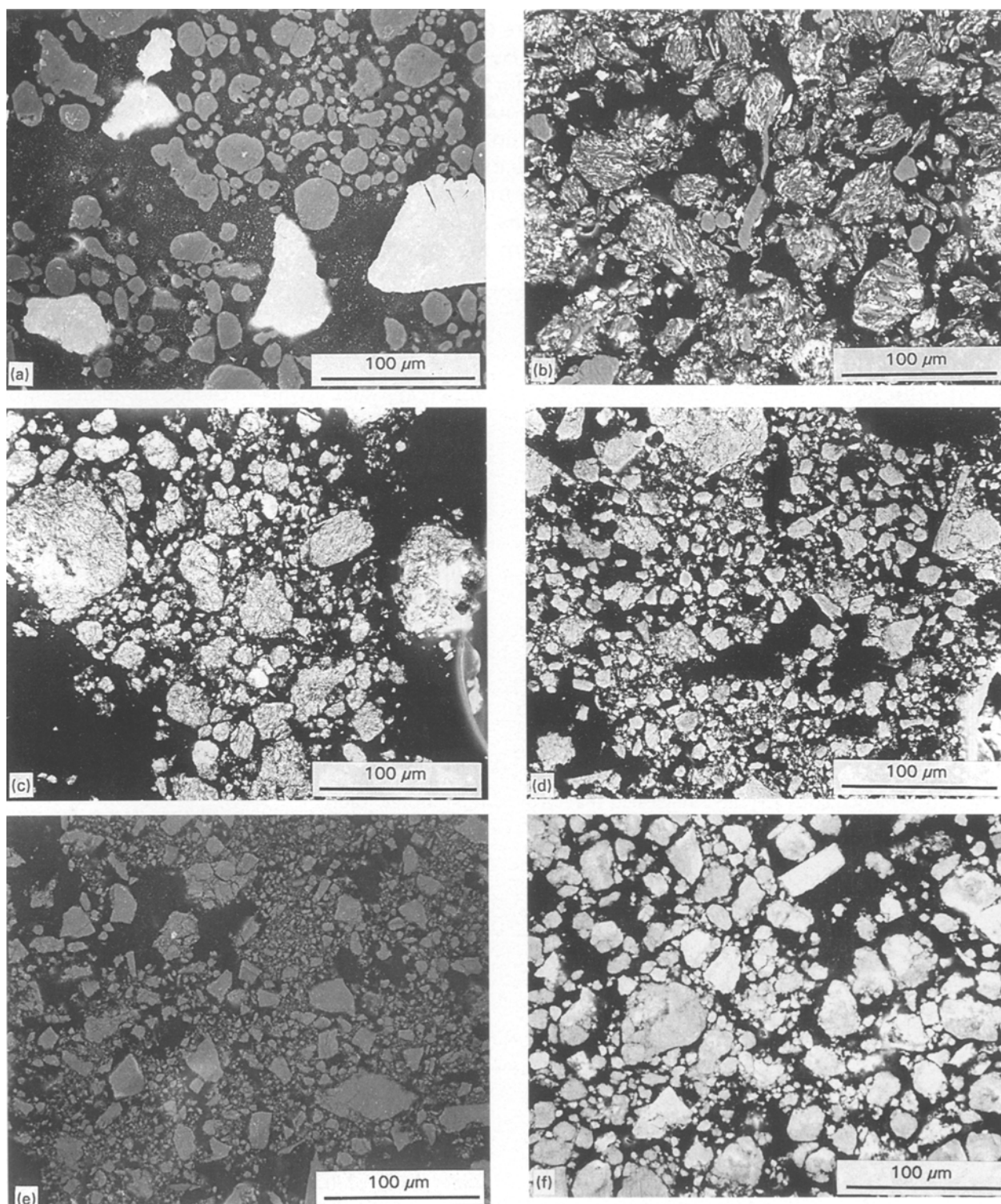


Figure 1 SEM micrographs of Al-10 at % Bi powder MA processed for (a) 0 h, (b) 1 h, (c) 3 h, (d) 5 h, (e) 10 h and (f) 20 h.

observations, samples were sliced by a microtome using a diamond blade. Changes in hardness were examined with MA time by measurements of the Vickers hardness. The thermal stabilities of the powders were investigated by differential scanning calorimetry (DSC, Perkin Elmer, DSC-7) at a heating rate of 0.33 Ks^{-1} .

3. Results

SEM micrographs of Al-10 at % Bi powder MA processed for various times are shown in Fig. 1. As

shown in Fig. 1a, the morphology of the starting Al (contrasted in black) and Bi (contrasted in white) powders are almost spherical particles. After 1 h of processing (initial stage of MA), the particles had developed into coarse particles with an average particle size of $70 \mu\text{m}$ due to the repetitive rolling and cold welding.

During the period from 3–5 h (second stage of MA), there is a substantial increase in the relative amount of equiaxed shaped grains. The particle size gradually decreased. The powders were hardened through repetitive deformation and fracturing of the powders occurred easily.

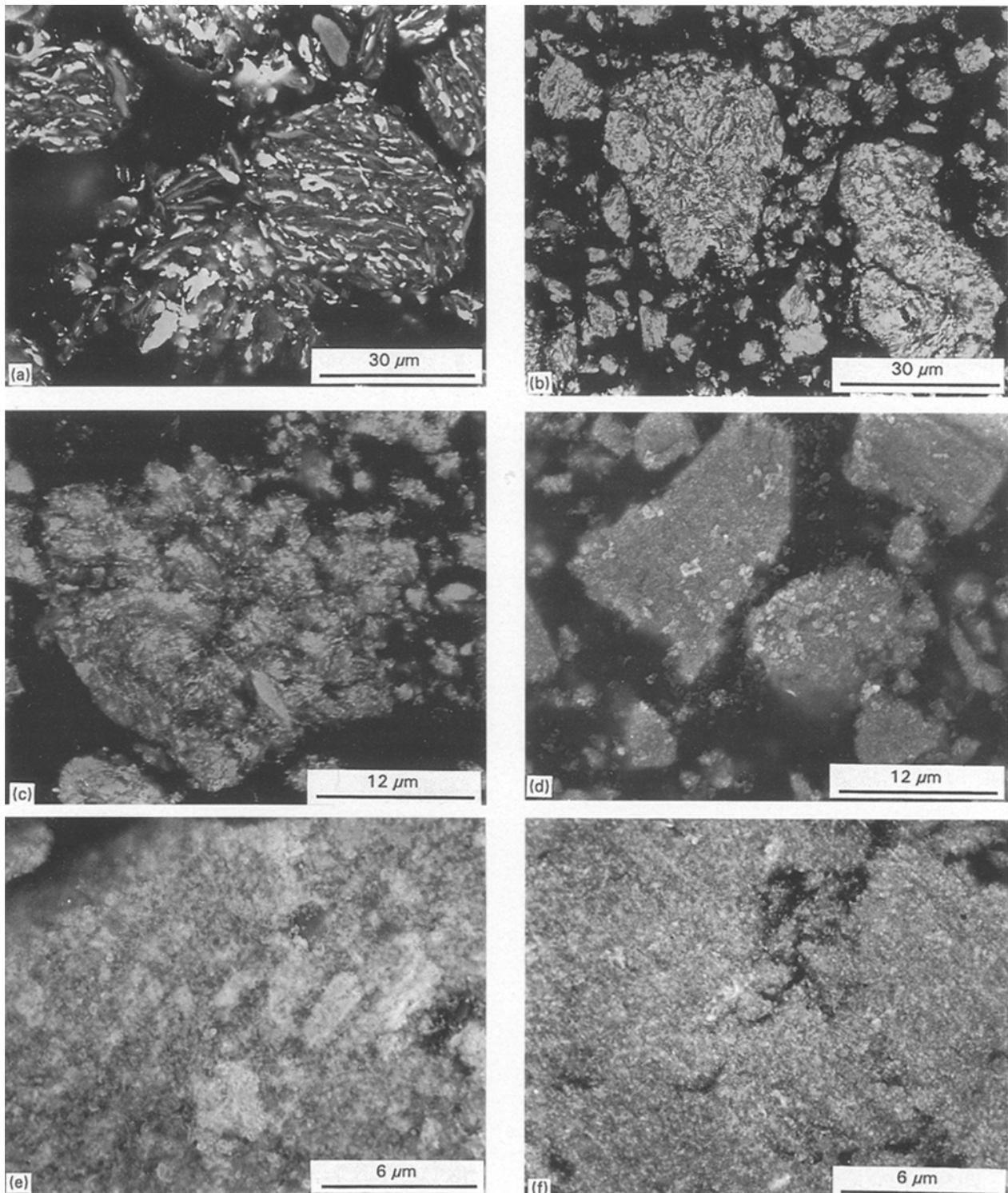


Figure 2 Changes in the microstructures of Al-10 at % Bi MA powder as a function of MA time, (a) 1 h, (b) 3 h, (c) 5 h, (d) 10 h, (e) 20 h and (f) 40 h.

For processing times longer than 10 h (third stage of MA), there was little distribution in the particle morphology. The MA powders were spherical. The balance between the fracturing and cold welding of the powders had reached a steady state.

Fig. 2 shows the changes in the microstructures of an Al-10 at % Bi MA powder as a function of MA time. As Al and Bi are ductile materials, both elements were deformed and the structure of the powders was lamellar. With increasing MA time, the lamellar spacing became smaller. The thickness of the Bi decreased faster than that of the Al powder because Bi is more ductile than Al. The MA powders increased their internal homogeneity by extensive fracturing and cold welding of the starting powders. Finally, each element was mixed in to sub-micrometer order.

Fig. 3 shows the TEM images of an Al-10 at % Bi powder mechanically alloyed for 160 h. As is evident from the bright and dark images, the Bi grains embedded in Al matrix were equiaxed and the grain size was about 30 nm. Fig. 4 shows the bright field TEM image of an Al-30 at % Bi powder mechanically alloyed for 160 h. Similarly to the behaviour observed in the Al-10 at % Bi powder, the Bi grains embedded in Al matrix were equiaxed and their size was about 50 nm. The grain size of the Al-30 at % Bi powder is thus larger than that of the Al-10 at % Bi powders. This difference in grain size can be interpreted as being due

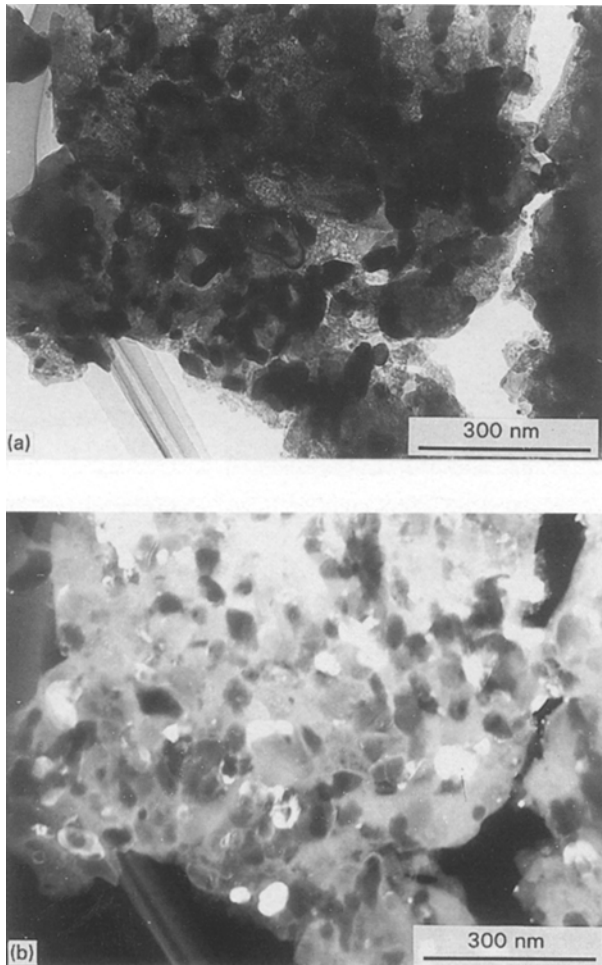


Figure 3 (a) Bright field and (b) dark field TEM micrographs of Al-10 at % Bi powder mechanically alloyed for 160 h.

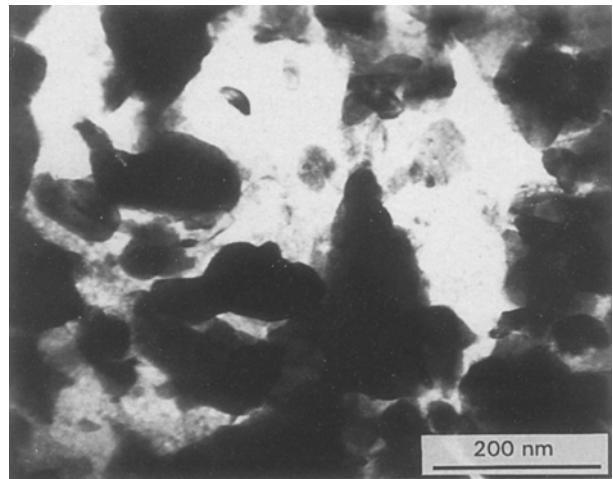


Figure 4 TEM micrograph of Al-30 at % Bi powder mechanically alloyed for 160 h.

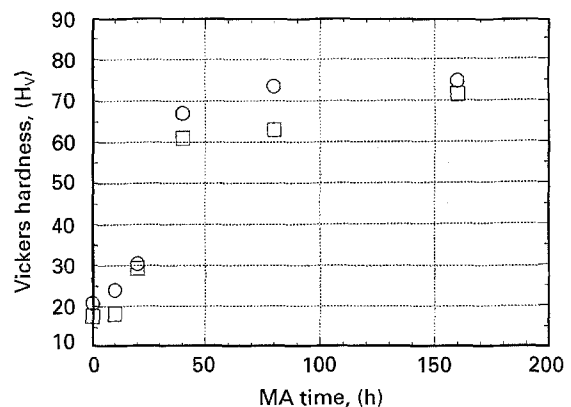


Figure 5 Changes in the Vickers hardness of MA powder as a function of MA time. The data were taken on (○) Al-10 at % Bi and (□) Al-30 at % Bi.

to the difference in processing rate. With increasing concentration of the Bi element, the powders become softer and the milling efficiency becomes smaller.

Fig. 5 shows the change of Vickers hardness, H_v , of MA powder for both compositions as a function of MA time. The hardness rapidly increased during the early stage of MA because of the reduction of grain size and deformation hardening, but with further MA it gradually reached a saturation value of 80 Hv. This maximum saturation value of H_v increased with an increase in the content of the harder Al in the starting powder and was much larger than that expected from the rule of mixing.

Fig. 6 shows the X-ray diffraction patterns of Al-10 at % Bi and Al-30 at % Bi MA powders mechanically alloyed for various times. The Bi peaks become slightly broader and shift to higher angles with processing time, whereas the intensities of the Al peaks decreased rapidly especially in the composition Al-30 at % Bi and no shift to higher angles were observed.

This obvious broadening of the diffraction peaks coupled with the decrease in the peak intensities is caused by the refinement in the grains and the observed shift of Bi peaks to higher diffraction angles is due to changes in the Bi lattice parameters.

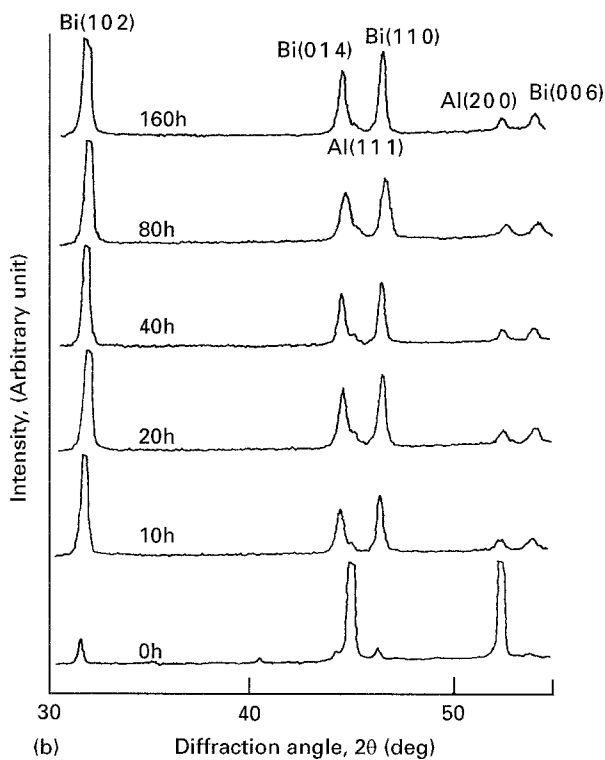
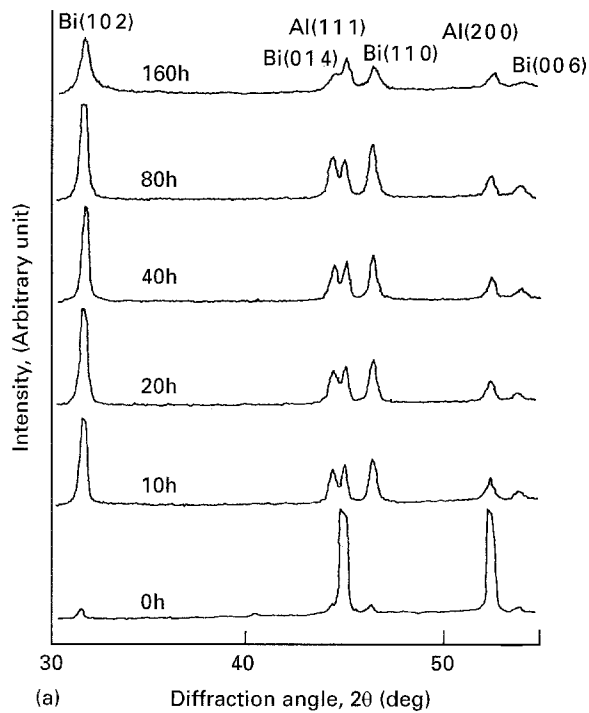


Figure 6 X-ray diffraction patterns of (a) Al-10 at % Bi and (b) Al-30 at % Bi MA powders mechanically alloyed for various times.

Fig. 7 shows the change in the average Bi grain size, which is calculated from the Scherrer formula [12] with the half-width of the Bi (110) diffraction peak, as a function of milling time. The crystallite size rapidly decreased in the early stage of MA and it gradually reached a minimum constant value. The saturation values of Bi crystallite size are about 25 nm and 30 nm for the Al-10 at % Bi and the Al-30 at % Bi alloys, respectively. These values are almost the same (or a little smaller) as those confirmed by TEM observation.

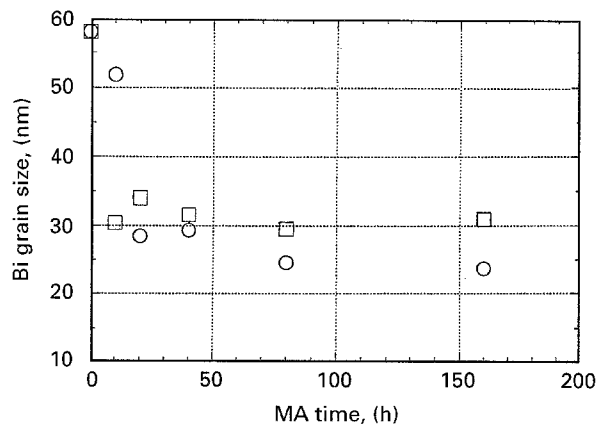


Figure 7 Change in average grain size of Bi calculated from the Scherrer formula with the half-width of the Bi (110) diffraction peak, as a function of milling time. The data were taken on: (○) Al-10 at % Bi and (□) Al-30 at % Bi.

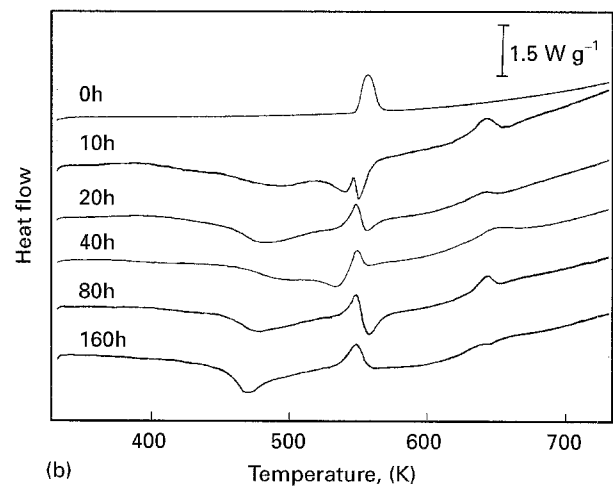
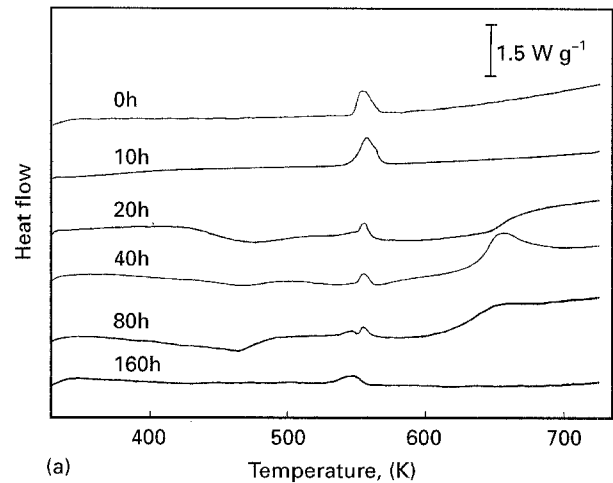


Figure 8 DSC curves of the (a) Al-10 at % Bi and (b) Al-30 at % Bi powder mechanically alloyed for various times.

Similar behaviour to that displayed by the crystallite size, is shown by the lattice parameter of Bi in that initially it decreased with the MA time and then reached a saturation value after 160 h of MA. The maximum change in the lattice parameter a , which is calculated from the Bi (110) peak, was at about -0.28% in the Al-10 at % Bi and -0.40% in the Al-30 at % Bi MA powders. The change in the c lattice parameter was roughly the same as that observed

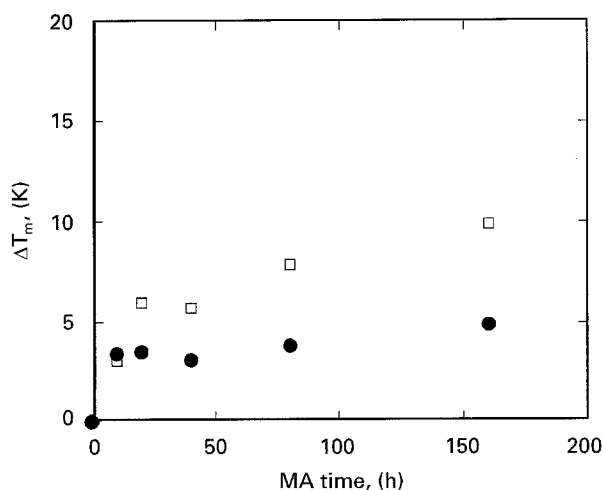


Figure 9 Changes in the melting temperature depression of Bi for mechanically alloyed (●) Al-10 at % Bi and (□) Al-30 at % Bi alloys as a function of MA time.

in the a parameter. The solubility of Al in Bi may be estimated from Vegard's law, to be about 0.7 at % in the Al-10 at % Bi alloy and 1.9 at % in Al-30 at % Bi. Both of these values are larger than the equilibrium solubility, which has been reported to be virtually nil.

Fig. 8 shows the changes in DSC curves of the MA powder as a function of MA time. We started with pure Bi which melted at 543 K but with increasing MA time, the melting temperature shifted to lower temperatures and the endothermic peak became broad. From about 400 K, a broad exothermic peak can be observed. This peak may be due to the decomposition of a super-saturated solid solution or to the release of a stored lattice distortion. The X-ray diffraction patterns of powders heated up to 400 K (before the exothermal peak) and to 500 K (after the peak), showed no significant changes and a reason for this exothermal peak could not be elucidated. Fig. 9 shows the changes in the melting temperature depression of Bi for mechanically alloyed Al-10 at % Bi and Al-30 at % Bi alloys as a function of MA time. With increasing the MA time, the temperature depression became larger and finally reached 4.9 K and 10.9 K for the Al-10 at % Bi and 30 at % Bi powders, respectively.

4. Discussion

The formation of a super-saturated solid solution in the Al-Bi system by MA was confirmed by the lattice parameters measurements. As discussed in the introduction, the heat of mixing in this system is positive. In such an alloy system, only the initial mixed state (state before MA) is a thermodynamically stable state, so the formation of solid solution means an elevation in the free energy by MA. This behaviour has been recently reported in some alloy systems and the energy was thought to be stored in the system as an interfacial energy of the nano crystals. The interfacial energy per unit volume increases proportionally to the reciprocal of the crystal size, so if the crystal size produced by MA becomes smaller, then the stored energy will be-

come larger. In the Fe-Cu alloy system where the crystal size produced by MA is less than 10 nm, the stored energy was more than 10 kJ mol^{-1} and non-equilibrium phases were formed over a wide composition range. In the present system, the crystal size of Al or Bi was about 30 nm due to the low milling efficiency, thus enough energy was stored that a super-saturated solid solution was formed over a wide composition. Extra application of the milling media thereby further reducing the crystal size will improve the solubility of the Al in the hcp Bi.

The obtained MA powders showed a depression of the melting temperature, which was more evident than in the case of the Al-In alloy system. As for the reasons why the melting temperature is depressed, two factors can be considered. One is the refinement of Bi crystallites and the other is the formation of a super-saturated hcp Bi solid solution.

It is generally known that there is a difference in the melting temperature between bulk and nano crystals because the surface area increases with decreasing the crystallite size and under these circumstances changes in the interfacial energy from solid to liquid cannot be neglected. According to Allen *et al.* [13], the melting temperature, T_{mf} of pure nanometer-sized crystals can be described as follows;

$$T_{mf}/T_o = 1 - K/r$$

T_o is the melting temperature of the bulk crystal and r the grain size. K is a constant value determined by the element and is about 0.08 nm in Bi.

In the case of nanocrystals embedded in an other element matrix, the T_{mf} can be estimated by the same equation. However, the constant value, K changes by taking the wetting angle of nanocrystals with the matrix into consideration [14]. There are no data concerning the wetting angle in Al-Bi alloy system, but by using the model of Miedema and Broeder [15], K can be estimated to be about 1.03 nm.

Since the grain size has been confirmed by XRD analysis and TEM observation to be 30 nm, the depression can be calculated to be about 19 K. This calculated value does not correspond with the observed one. Moreover, such a large difference in the depressed temperature between Al-10 at % Bi and Al-30 at % Bi, 5 K, can not be interpreted by this factor while the grain sizes are similar in size.

Fig. 10 shows the Al-Bi phase diagram in the Bi rich side. By lattice parameter measurements, the enhanced solid solubilities are estimated to be 0.7% Al and 1.9% Al in the composition of Al-10 at % Bi and Al-30 at % Bi, respectively. From the extrapolation of the solidus line, the melting temperature of the super-saturated solid solution can be evaluated. The solubility of Al in Bi at the eutectic temperature has not been reported. If it is assumed to be 0.15%, the depressed temperature estimated by this procedure corresponded well with that measured by DSC analyses.

These results show that the depression of the melting temperature is more dependent on the super-saturated solubility than on grain size factors. In previous work concerning the MA of Al-In alloy system,

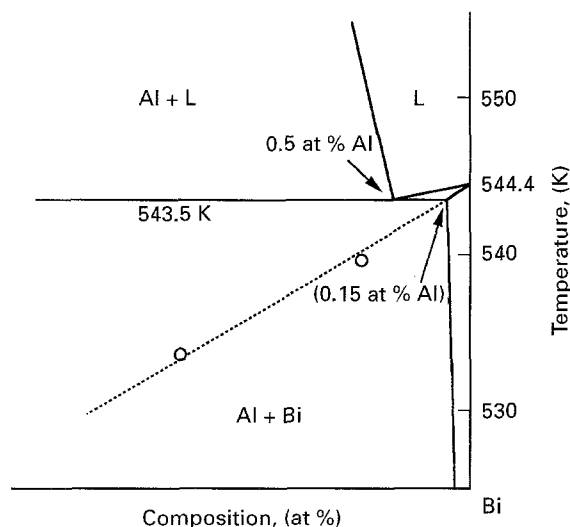


Figure 10 Al-Bi phase diagram for Bi rich compositions. Broken line is an extrapolated solidus line.

such a depression in the melting temperature was observed and was shown to be related not to refinements of In crystallites but to the formation of super-saturated fct. In solid solution [11]. In the Al-Bi system, the depression of melting temperature is also caused by the formation of a super-saturated solid solution, in this case a hcp Bi solid solution.

5. Conclusions

Mechanical alloying by vibrating ball milling was performed on the immiscible Al-Bi alloy system. The alloying behaviours were investigated by SEM and TEM observation, XRD analysis, hardness measurements and DSC studies.

The results obtained in this work are as follows;

(1) Al and Bi were mixed finely and homogeneously with increasing MA time, and the grain size was lowered to 30 nm by MA for 160 h.

(2) The hardness of MA powders increased with MA time up to 70 Hv, a value which is much larger than that calculated from the rule of mixing.

(3) Lattice parameter measurements of Bi by X-ray diffraction analysis, show that the solubility of Al in Bi

was about 1.9% at % in Al-30 at % Bi which is larger than that in the equilibrium state.

(4) The melting temperature of Bi was confirmed to be depressed by the formation of a hcp Bi super-saturated solid solution. The maximum depression in the temperature was about 10 K, which corresponded well with the value estimated by the extrapolation of the solidus line.

Acknowledgements

The authors thank Dr. T. Tanaka, Osaka Sangyo University, for experimental help in the sample preparation for TEM observation.

References

1. J. S. BENJAMIN, *Metall. Trans.* **1** (1970) 2943.
2. P. S. GILMAN and J. S. BENJAMIN, *Ann. Rev. Mater. Sci.* **13** (1983) 1791.
3. C. C. KOCH, O. B. CAVIN, C. G. MCKAMEY and J. O. SCARBROUGH, *Appl. Phys. Lett.* **43** (1983) 1017.
4. R. B. SCHWARZ, R. R. PETRICH and C. K. SAW, *J. Non-Cryst. Solids* **76** (1985) 281.
5. E. HELLSTERN, L. SCHULTZ, R. BORNEMANN and D. LEE, *Appl. Phys. Lett.* **53** (1988) 1399.
6. B. T. MCDERMOTT and C. C. KOCH, *Scripta Metall.* **20** (1986) 669.
7. J. S. BENJAMIN and T. E. VOLIN, *Metall. Trans.* **5** (1974) 1929.
8. K. UENISHI, K. F. KOBAYASHI, K. N. ISHIHARA and P. H. SHINGU, *Mater. Sci. & Eng.* **A134** (1991) 1342.
9. K. UENISHI, K. F. KOBAYASHI, S. NASU, H. HATANO, K. N. ISHIHARA and P. H. SHINGU, *Z. Metallkde.* **83** (1992) 132.
10. K. UENISHI, K. F. KOBAYASHI, K. N. ISHIHARA and P. H. SHINGU, *Mater. Sci. Forum* **88-90** (1992) 459.
11. K. UENISHI, H. KAWAGUCHI and K. F. KOBAYASHI, *J. Mater. Sci.* **29** (1994) 4860.
12. B. D. CULITY, "Elements of X-ray diffraction" (Addison Wesley, USA, 1987) 102.
13. G. L. ALLEN, W. W. GILE and W. A. JESSER, *Acta Metall. Mater.* **28** (1980) 1695.
14. H. SAKA, *Bull. Jpn Inst. Met.* **31** (1992) 204.
15. A. R. MIEDEMA and F. J. A. DEN BROEDER, *Z. Metallkde.* **70** (1979) 14.

Received 28 June 1995

and accepted 21 December 1995